ISSN 1990-4789, Journal of Applied and Industrial Mathematics, 2018, Vol. 12, No. 4, pp. 1–14. © Pleiades Publishing, Ltd., 2018.
Original Russian Text © I.V. Vasil'ev, M.V. Vasilieva, V.S. Gladkikh, V.P. Ilin, D.Ya. Nikiforov, D.V. Perevozkin, G.A. Prokopev, 2018, published in Sibirskii Zhurnal Industrial'noi Matematiki, 2018, Vol. XXI, No. 4, pp. 15–27.

Numerical Solution of a Fluid Filtration Problem in a Fractured Medium Using Domain Decomposition Method

V. I. Vasil'ev[1*], M. V. Vasil'eva[1], V. S. Gladkikh[2***], V. P. Ilin[2,3****], D. Ya. Nikiforov[1*****], D. V. Perevozkin[2******], and G. A. Prokop'ev[1*******]**

[1] *Ammosov North-Eastern Federal University, ul. Belinskogo 58, Yakutsk, 677000 Russia*

[2] *Institute of Computational Mathematics and Mathematical Geophysics, pr. Akad. Lavrent'eva 6, Novosibirsk, 630090 Russia*

[3] *Novosibirsk State University, ul. Pirogova 2, Novosibirsk, 630090 Russia*

Received June 18, 2018

Abstract—Under consideration are the numerical methods for simulation of a fluid flow in a fractured porous media. The fractures are taken into account explicitly using a discrete fracture model. The formulated single-phase filtering problem is approximated by an implicit finite element method on unstructured grids that resolve fractures at the grid level. The systems of linear algebraic equations (SLAE) are solved by the iterative methods of domain decomposition in the Krylov subspaces using the KRYLOV library of parallel algorithms. The results of solving some model problem are presented. A study is conducted of the efficiency of the computational implementation for various values of contrast coefficients, which significantly affect the condition number and the number of iterations required for convergence of the method.

DOI: 10.1134/S1990478918040014

Keywords: *filtering, fractured medium, discrete fracture model, approximation, flow rate, finite element method, unstructured grid, iterative method*

INTRODUCTION

When developing some oil and gas fields, a realistic description is necessary of the fluid behavior in the reservoir. From this point of view, description of fractures in explicit form is more accurate compared to traditional dual porosity models [1]. One of these methods is the discrete fracture model (DFM) in which it is assumed that fractures have a dominant effect on fluid flows. Although the total volume of fractures is very small, but, since their aperture is low and oil is not stored in them in practice, the main

*E-mail: vasvasil@mail.ru
**E-mail: vasilyevadotmdotv@gmail.com
***E-mail: gladvs_ru@mail.ru
****E-mail: ilin@sscc.ru
*****E-mail: dju92@mail.ru
******E-mail: foxillys@gmail.com
*******E-mail: khloros35@gmail.com

flow occurs exactly along the fractures due to greater permeability. Usually, the fractures are represented explicitly by the objects of dimension of an order of magnitude lower than that of the reservoir [2–5].

The fracture discrete model is considered as a method which is well-applicable for a formation with low degree of the fracture development, especially when the reservoir has several large cracks which control the flow direction. The conceptual model of discrete fractures was introduced in [6]. A model that is currently actively applied is presented in [7], where the problem was solved by using the finite element method, while assuming that the porous medium is a two-dimensional plane, whereas the fractures are one-dimensional lines with high permeability. Application of a discrete model of fractures and methods for the numerical solution of two-phase filtration problems is considered in [6–15].

After approximation of the differential problem, it is necessary to solve SLAE with large number of unknowns. Due to the presence of fractures, the problem under consideration becomes identical to the problem with highly inhomogeneous coefficients. Consequently, the condition number of the resulting matrix increases due to the large difference between the permeability coefficients of the porous medium and the fracture network; and the greater the difference between the coefficients, the greater the condition number becomes. It is well-known that the matrix condition number directly affects the number of iterations when solving a system of equations by the iterative methods.

The article deals with numerical studying the features of a solution of the SLAE resulting from the implicit finite element approximation of a poorly conditioned problem using the iterative methods of domain decomposition in the Krylov subspaces [16]. In the numerical implementation of SLAE we used the two-level iterative methods from the KRYLOV library of parallel algorithms [17–23]. To solve the problems under study, the Schwartz additive method is used that acts as a preconditioner for the original matrix in the FGMRes method. We present the results of numerical experiments with different contrast of the permeability coefficients of the porous media and fractures.

1. STATEMENT OF THE PROBLEM

Consider the continuity equation in a domain $\Omega \in \mathbb{R}^d$ describing the single-phase motion of a fluid in a porous medium:

$$\frac{\partial(\varphi\rho)}{\partial t} + \operatorname{div}(\rho u) = 0, \qquad \mathbf{x} \in \Omega, \qquad 0 < t \le T < \infty, \tag{1}$$

where φ is the reservoir porosity, ρ is the fluid density, p is pressure, $k = k(\mathbf{x})$ is the permeability tensor of the porous medium, μ is the fluid viscosity, u is the flow velocity of the fluid described by the Darcy's law

$$u = -\frac{k}{\mu} \operatorname{grad} p, \qquad \mathbf{x} \in \Omega. \tag{2}$$

Since the fracture thickness is several orders of magnitude smaller than the size of Ω, consideration of fractures at the grid level leads to the problems of large dimensions. We consider further an alternative approach used for studying the filtering problems in fractured media. This approach is based on the representation of cracks by a special interface condition on some inner boundary γ of the domain $\Omega \subset \mathbb{R}^d$, where $d = 2, 3$.

Usually, the fracture Ω_f is rather thin, and so, following [24], we can replace the d-dimensional equation in $\Omega_f \subset \mathbb{R}^d$ by some $(d-1)$-dimensional equation on the surface $\gamma \subset \mathbb{R}^{d-1}$ by integrating the mass conservation equations and the Darcy's law over the fracture thickness. Let the fracture have thickness $b = b(s)$ and

$$\Omega_f = \{x \in \Omega \mid x = s + en_f,\ s \in \gamma,\ -b/2 < e < b/2\},$$

where γ is a smooth surface, and n_f is the normal to γ. We integrate the mass conservation equation over the thickness and write it as the equation on the surface γ:

$$\int\limits_{-b/2}^{b/2} \frac{\partial(\varphi\rho)}{\partial t}\, dn_f + \int\limits_{-b/2}^{b/2} \operatorname{div}_\tau u\, dn_f + \int\limits_{-b/2}^{b/2} \operatorname{div}_{n_f} u\, dn_f = \int\limits_{-b/2}^{b/2} f\, dn_f,$$

where div_τ and div_{n_f} stand for the operators of tangential and normal divergence on γ respectively;

$$f = \sum_i q_i \delta_\varepsilon(\mathbf{x} - \mathbf{x}_i)$$

is the cumulative intensity of sources/sinks in the neighborhood of $\mathbf{x}_i$; q_i is the intensity of the ith source/sink, where

$$\delta_\varepsilon(\mathbf{x} - \mathbf{x}_i) = \begin{cases} 1/(\pi\varepsilon^2), & |x - x_i| \le \varepsilon, \\ 0, & |x - x_i| > \varepsilon, \end{cases}$$

and ε is the well radius.

Let p_f and u_f be the average pressure and velocity along γ:

$$p_f = \frac{1}{b} \int\limits_{-b/2}^{b/2} p\, dn_f, \qquad u_f = \int\limits_{-b/2}^{b/2} u_{f,\tau}\, dn_f,$$

where $u = u_{f,n_f} + u_{f,\tau}$, while u_{f,n_f} and $u_{f,\tau}$ are the normal and tangential components of the velocity. Since

$$\int\limits_{-b/2}^{b/2} \operatorname{div}_{n_f} u\, dn_f = [u \cdot n_f], \qquad [u \cdot n_f] = u^+ \cdot n_f - u^- \cdot n_f,$$

where u^+ and u^- are the velocity values to the left and to the right of γ, we have the following equation on γ:

$$\frac{\partial(\varphi\rho)}{\partial t} + \operatorname{div}_\tau u_f + [u \cdot n_f] = f, \qquad \mathbf{x} \in \gamma. \tag{3}$$

The Darcy's law can be written as follows:

$$u_{f,\tau} = -\frac{k_{f,\tau}}{\mu} \operatorname{grad}_\tau p_f, \qquad u_{f,n_f} = -\frac{k_{f,n_f}}{\mu} \operatorname{grad}_{n_f} p_f, \tag{4}$$

where k_{f,n_f} and $k_{f,\tau}$ are the normal and tangential components of the permeability coefficient k_f. Integrating (4) over the fracture thickness, we infer that

$$u_f = -b\frac{k_{f,\tau}}{\mu} \operatorname{grad}_\tau p_f, \qquad \mathbf{x} \in \gamma, \tag{5}$$

$$\{u \cdot n_f\} = -\frac{k_{f,n_f}}{b\mu} [p], \qquad \mathbf{x} \in \gamma, \tag{6}$$

$[p] = (p^+ - p^-)$ is the pressure jump, and $\{u \cdot n_f\} = (u^+ \cdot n_f + u^- \cdot n_f)/2$ is the average velocity.

To determine the average pressure along the fracture, we can use the linear approximation as

$$p_f = \{p\} + \frac{d\mu}{k_{f,n_f}}[u \cdot n_f], \qquad x \in \gamma. \tag{7}$$

Thus, we obtain the connected system of equations described by the d-dimensional equation (1) in the domain Ω and $(d-1)$-dimensional equation in the fracture with some internal source depending on the flow from the matrix of the porous medium into the fractures:

$$\begin{gathered}\frac{\partial \varphi_f \rho}{\partial t} + \operatorname{div}_\tau u_f + [u \cdot n_f] = f, \qquad \mathbf{x} \in \gamma, \\ u_f = -b\frac{k_{f,\tau}}{\mu}\operatorname{grad}_\tau p_f, \qquad \mathbf{x} \in \gamma,\end{gathered} \tag{8}$$

where b is the thickness of the fracture, k_f is the permeability of the fractures, while p_f and u_f stand for the pressure and velocity of the fluid flow respectively. The derivation and description of the model under consideration can be found in [24–29] in more detail.

In what follows, we will consider the case of an incompressible fluid flow $\rho = \mathrm{const}$ in an elastic deformable porous medium:

$$\frac{\partial \varphi}{\partial t} = c_r \varphi_0 \frac{\partial p}{\partial t}, \tag{9}$$

where φ_0 is the porosity at some given p_0, and c_r is the compressibility of the porous medium.

Inserting the Darcy's law (2) into the continuity equation (1), we arrive to the following parabolic equation that is resolved with respect to pressure [1, 30]:

$$c\frac{\partial p}{\partial t} - \operatorname{div}\left(\frac{k}{\mu}\operatorname{grad} p\right) = 0, \qquad \mathbf{x} \in \Omega, \tag{10}$$

where $c = c_r\varphi_0$.

By analogy, for the flow in the fracture network, we obtain

$$c_f\frac{\partial p_f}{\partial t} - \operatorname{div}\left(b\,\frac{k_f}{\mu}\operatorname{grad} p_f\right) + [u \cdot n_f] = f, \qquad \mathbf{x} \in \gamma. \tag{11}$$

Note that the flow exchange between the fracture and the matrix of porous medium is also present in the equation for the matrix of the porous medium in the form of an interface condition which appears in the problem approximation. (This model of mixed dimension describing the flow in a fractured porous medium is widely known [24–29].)

Let us complement (10) with the initial condition, the Neumann boundary condition, and the interface condition:

$$p(\mathbf{x}, 0) = p_0(\mathbf{x}), \quad \mathbf{x} \in \Omega, \qquad p_f(\mathbf{x}, 0) = p_0(\mathbf{x}), \quad \mathbf{x} \in \gamma, \tag{12}$$

$$u \cdot \mathbf{n} = 0, \quad \mathbf{x} \in \partial\Omega, \qquad u_f \cdot \mathbf{n} = 0, \quad \mathbf{x} \in \partial\gamma, \tag{13}$$

$$\{u \cdot n_f\} = -\sigma(p - p_f), \qquad \sigma = k_{f,n_f}/(b\mu), \quad x \in \gamma, \tag{14}$$

where $\mathbf{n}$ is the outer normal to the boundary of the domain.

2. FINITE-ELEMENT APPROXIMATION

Consider a spatial discretization by the finite element method for the systems of equations (10) and (11) with interface condition (14). To approximate the fractures, we use the discrete model of cracks [25]. This approach is based on the representation of fractures on an unstructured grid by the faces of finite elements.

Let $\mathcal{T}_h$ be some partition of the domain into the elements K (*grid cells*). In the case of highly permeable fractures, we assume that $p^+ = p^- = p_f$ [24] and

$$\int\limits_K \nabla \cdot u\, z\, dx = -\int\limits_K u \cdot \nabla z\, dx + \int\limits_\gamma [u \cdot n_f] z\, ds.$$

Then, taking into account the interface conditions for the matrix of the porous medium, we arrive at

$$\int\limits_\Omega c\frac{\partial p}{\partial t} z\, dx + \int\limits_\Omega \left(\frac{k}{\mu} \operatorname{grad} p, \operatorname{grad} z\right) dx - \int\limits_\gamma [u \cdot n_f] z\, ds = 0 \tag{15}$$

and for the fractures

$$\int\limits_\gamma c_f \frac{\partial p_f}{\partial t} z_f\, ds + \int\limits_\gamma \left(b\frac{k_f}{\mu} \operatorname{grad} p_f, \operatorname{grad} z_f\right) ds + \int\limits_\gamma [u \cdot n_f] z_f\, ds = \int\limits_\gamma f z_f\, ds. \tag{16}$$

For $p_f = p$, using the superposition method, we have

$$\begin{aligned} &\int\limits_\Omega c\frac{\partial p}{\partial t} z\, dx + \int\limits_\Omega \left(\frac{k}{\mu} \operatorname{grad} p, \operatorname{grad} z\right) dx \\ &\qquad + \sum_j \left(\int\limits_{\gamma_j} c_f \frac{\partial p}{\partial t} z_f\, ds + \int\limits_{\gamma_j} \left(b\frac{k_f}{\mu} \operatorname{grad} p, \operatorname{grad} z_f\right) ds\right) = \sum_j \int\limits_{\gamma_j} f z_f\, ds, \end{aligned} \tag{17}$$

where $j = \overline{1, M_f}$ and M_f is the number of discrete fractures. The derivation of the approximation can be found in [25] in more detail.

For approximation in time we use a purely implicit discretization of the equations

$$\begin{aligned} &\int\limits_{\Omega_m} c\frac{p^{n+1} - p^n}{\tau} z\, dx + \sum_i \int\limits_{\gamma_i} c_f \frac{p^{n+1} - p^n}{\tau} z_f\, ds + \int\limits_\Omega \left(\frac{k}{\mu} \operatorname{grad} p^{n+1}, \operatorname{grad} z\right) dx \\ &\qquad + \sum_i \int\limits_{\gamma_i} \left(b\frac{k_f}{\mu} \operatorname{grad} p^{n+1}, \operatorname{grad} z_f\right) ds = \sum_i \int\limits_{\gamma_i} f^n z_f\, ds, \end{aligned} \tag{18}$$

where γ_i is the domain of crack i, τ is the time step, and n is the number of the time layer.

We will use the simplest continuous linear finite functions of the first order as the basis functions. To use the standard Galerkin method, we write the solution of the problem and test functions in the form

$$p_h = \sum_{i=1}^N p_i \varphi_i, \qquad v_h = \sum_{i=1}^N \varphi_i,$$

where φ_i are piecewise-linear basis functions, whereas N is the number of nodes in the computational grid $\mathcal{T}_h$. Thus, (18) is reduced to the system of algebraic equations

$$(M + \tau A) p^{n+1} = M p^n, \tag{19}$$

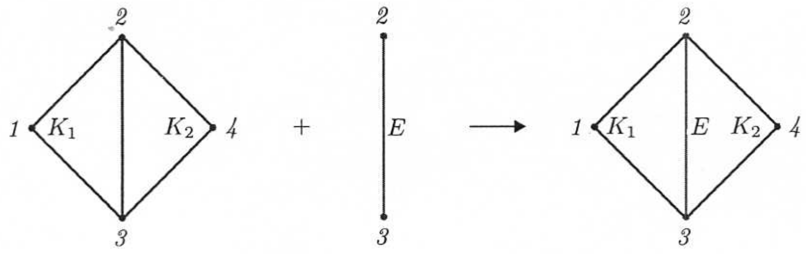

Fig. 1. DFM approximation.

M and A are symmetric matrices of mass and rigidity respectively having the form

$$M = \left\{ m_{ij} = \int\limits_{\Omega} c\varphi_i\varphi_j \, dx + \sum_k \int\limits_{\gamma_k} c_f \psi_i \psi_j \, dx \right\},$$

$$A = \left\{ a_{ij} = \int\limits_{\Omega} \frac{k}{\mu} \nabla\varphi_i \cdot \nabla\varphi_j \, dx + \sum_k \int_{\gamma_k} \frac{k_f}{\mu} \nabla\psi_i \cdot \nabla\psi_j \, dx \right\},$$

where ψ_i are the linear basis functions defined only on the fractures.

To illustrate the DFM method by an example, we consider approximation of the matrix of the mass in the case of two triangular finite elements K_1 and K_2 on whose intersection there is some one-dimensional fracture E (see Fig. 1). Here the elements of the matrix have the following form:

$$m_{ij}^{K_1} = \int\limits_{K_1} c\varphi_i\varphi_j \, dx, \quad i, j = 1, 2, 3, \qquad m_{ij}^{K_2} = \int\limits_{K_1} c\varphi_i\varphi_j \, dx, \quad i, j = 2, 3, 4,$$

$$m_{ij}^{E} = \int\limits_{E} c_f \psi_i \psi_j \, dx, \quad i, j = 2, 3.$$

These quantities together form the elements of local mass matrices:

$$\begin{bmatrix} m_{11}^{K_1} & m_{12}^{K_1} & m_{13}^{K_1} & 0 \\ m_{21}^{K_1} & m_{22}^{K_1} + m_{22}^{K_2} & m_{23}^{K_1} + m_{23}^{K_2} & m_{24}^{K_2} \\ m_{31}^{K_1} & m_{32}^{K_1} + m_{32}^{K_2} & m_{33}^{K_1} + m_{33}^{K_2} & m_{34}^{K_2} \\ & m_{42}^{K_2} & m_{43}^{K_2} & m_{44}^{K_2} \end{bmatrix} + \begin{bmatrix} 0 & 0 & 0 & 0 \\ 0 & m_{22}^{E} & m_{23}^{E} & 0 \\ & m_{32}^{E} & m_{33}^{E} & 0 \\ 0 & 0 & 0 & 0 \end{bmatrix}$$

$$= \begin{pmatrix} m_{11}^{K_1} & m_{12}^{K_1} & m_{13}^{K_1} & 0 \\ m_{21}^{K_1} & m_{22}^{K_1} + m_{22}^{K_2} + m_{22}^{E} & m_{23}^{K_1} + m_{23}^{K_2} + m_{23}^{E} & m_{24}^{K_2} \\ m_{31}^{K_1} & m_{32}^{K_1} + m_{32}^{K_2} + m_{32}^{E} & m_{33}^{K_1} + m_{33}^{K_2} + m_{33}^{E} & m_{34}^{K_2} \\ 0 & m_{42}^{K_2} & m_{43}^{K_2} & m_{44}^{K_2} \end{pmatrix}$$

3. SOLUTION OF ALGEBRAIC SYSTEMS

At each step n of numerical integration in time of the original initial boundary value problem, it is necessary to solve a SLAE of type (19). This procedure is carried out iteratively until the condition of sufficient smallness of the Euclidean norm of the residual vector be fulfilled:

$$\|r^{n+1,k}\| \leq \varepsilon_n \|r^{n+1,0}\|, \qquad \varepsilon_n \ll 1, \qquad k = 1, \dots, m_{n+1}, \tag{20}$$

where k is the number of the current iteration and

$$r^{n+1,k} = f^n - \left(\frac{1}{\tau}M + A\right)p^{n+1,k}, \qquad f^n = g - \frac{1}{\tau}Mp^n. \tag{21}$$

By (21), the following relationship holds [19] for an approximate solution $p_\varepsilon^{n+1} = p^{n+1,m+1}$ of algebraic system (19):

$$\frac{1}{\tau}M + Ap_\varepsilon^{n+1} = g + \frac{1}{r}Mp^n - r_\varepsilon^{n+1}, \qquad r_\varepsilon^{n+1} = r_\varepsilon^{n+1,m_n}. \tag{22}$$

On the other hand, the following equality is fulfilled for the vector $(p)_h^{n+1}$ whose components are the values of the exact solution at the nodes of the space-time grid:

$$\left(\frac{1}{\tau}M + A\right)p_h^{n+1} = g + \frac{1}{\tau}Mp_h^n + \psi^n, \tag{23}$$

where $\psi^n = \psi_\tau^n + \psi_n^n = O(\tau + h)$ is the vector of the total temporal and spatial approximation errors. Hence, for the vector of the total error of the numerical solution z^{n+1} we have

$$\left(\frac{1}{\tau}M + A\right)z^{n+1} = \frac{1}{\tau}Mz^n + \psi^n + r_\varepsilon^{n+1}, \qquad z^{n+1} = p_h^{n+1} - p_\varepsilon^{n+1}. \tag{24}$$

From this the recurrent inequalities for the vector norms follow:

$$\|z^{n+1}\| \leq \|(I + \tau M^{-1}A)^{-1}\| \big(\|z^n\| + \tau\|M\| \cdot \|\psi^n + r_\varepsilon^{n+1}\|\big), \tag{25}$$

whence under natural assumptions on the positive semi-definiteness of $M^{-1}A$ and boundedness of the norm of M^{-1}, the boundedness of the error norm $\|z^{n+1}\|$ follows in the numerical integration of the original problem in some bounded time interval because $n = T/\tau$.

Owing to the relations under consideration, we need to perform balancing between the values of spatial and temporal approximations, and also the final discrepancy of the iterative solution of the SLAE for each n. An important question for reducing the number of iterations m_n is the choice of an appropriate initial approximation $p^{n+1,0}$. For sufficiently small gridsize τ, the simplest method is to define $p^{n+1,0} = p^n$. A natural development of this approach consists in using some predictor-corrector scheme; i.e., firstly, apply an explicit scheme instead of (19):

$$p^{n+1} = p^n + \tau M^{-1}(g - Ap^n). \tag{26}$$

To solve the given rather large SLAU with the sparse matrix stored initially in a compressed format (specifically, Compressed Sparse Row, CSR) in the memory of one processor, the KRYLOV library is applied. This includes the following technological stages:

1. Balanced algebraic-geometric decomposition of the computational domain (with some given number of grid layers of intersection of the subregions); i.e., in fact, conducting the partition of the matrix into the block rows of about the same size and distribution of the so-obtained subsystems among various MPI processes with simultaneous modification of the near-boundary equations to implement

various types of the interface conditions (Dirichlet, Neumann, or Newton-Robin) on adjacent nodes of the contacting subdomains.

2. The organization of synchronous solution of the formed algebraic subsystems in the subdomains on the corresponding multi-core processors with the implementation of "internal" parallelization using multi-threaded computations, wherein the preconditioned iteration algorithms in the Krylov subspaces are used, and the interface data is buffered for the preparation of subsequent economical exchanges between the neighboring MPI processes.

3. Execution of the external iterative process for the subdomains based on the block method of Schwarz–Jacobi in the Krylov subspaces using the accelerating procedures of coarse-grid correction or aggregation based on some low-rank approximation of the original matrix.

It is obvious that, in multiple solving of SLAE at different time steps, the repeated procedures are performed once before the start of the main calculations. It is also natural that, in mass calculations of the problems of the same type, the optimal planning of a machine experiment requires the preliminary studies on selection of the algorithmic parameters with the development of practical recommendations which can significantly improve the efficiency of simulation.

4. NUMERICAL STUDY OF THE SIMULATION RESULTS

Let us consider the numerical solution of the problem (10)–(13) of single-phase filtration with some network of fractures in the two-dimensional and three-dimensional settings. The porous medium is assumed homogeneous, but due to the presence of fractures the entire domain Ω is highly inhomogeneous. The difference between the permeability of the porous medium and that of fractures defines this inhomogeneity. Let $\eta = k_f/k$ be the parameter of the medium inhomogeneity. To study the effect of η on the convergence of the iterative method, we consider various values $\eta = 10^5$, 10^6, 10^7, and 10^8, and increase only k_f according to the formula $k_f = k\eta$. Assume that the thickness α_i of fracture i is identical for all i, namely, let $\alpha = 0.01$ m.

The approximation of equations and the construction of matrices is carried out on the FEniCS computing platform [13] with open source code (LGPLv3). The solution of SLAE is implemented by the two-level iterative processes in the Krylov subspaces with a preconditioner which is constructed by using the additive Schwartz method and the decomposition of the computational domain (with parallel calculations) with parameterized intersection of subdomains and implemented in the KRYLOV library [17–19]. As the external and internal iterative method we use FGMRES; the Eisen preconditioner is used in the subdomains (a modification of the Eisenstadt incomplete factorization algorithm).

For numerical experiments, we take the following input data: $\varphi_m = 0.4$, $\varphi_f = 1$, $c_R = 10^{-9}\,\mathrm{Pa}^{-1}$, $k = 10^{-15}\,\mathrm{m}^2$, $\mu = 2 \cdot 10^{-3}\,\mathrm{Pa}\cdot\mathrm{s}$, $\tau = 1$ day, and $p_0 = 10$ MPa.

5.1. Numerical Study in Two-Dimensional Case

In this study we use the model of a real formation located in northwestern China [21]. We consider the problem in the two-dimensional formulation with one source, which simulates a well (Fig. 2, a). The domain is the square with the sides of 4 km and has a network of fractures. We construct the grid with 13568 vertices and 26814 triangular elements (Fig. 2, b) using the free software Gmsh [27]. The grid is constructed so that the fractures are the faces of triangular elements.

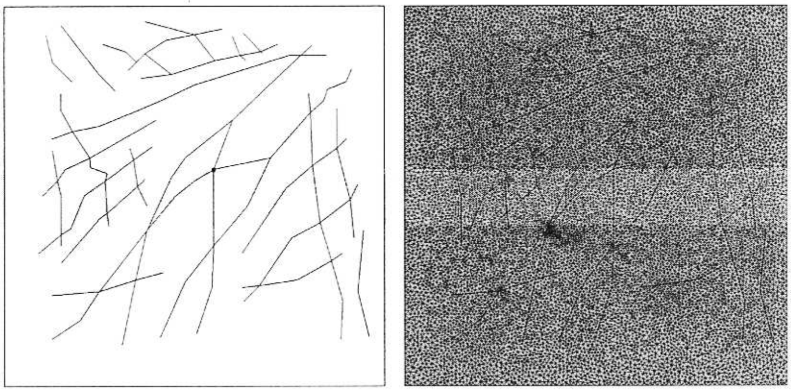

(a) (b)

Fig. 2. Geometry and grid in $2D$.

Table 1. Average number of iterations N_{iter} depending on η

η	1	2	3	4
N_{iter}	3.11	6.12	19.35	53

The right-hand side in (10) is the source $f = -PI(p^n(x) - p_b)$ ($p_b = 10^5$ Pa is the bottom hole pressure, and PI is the Pisman coefficient) and has the form

$$PI = \frac{2\pi k H_3}{\mu \log(r_e/r_w)}, \tag{27}$$

where $r_w = 0.1$ m is the radius of the well, $r_e = He^{-\pi/2} \approx 0.20788H$ is the equivalent radius (Pisman radius or the feed contour radius of the well), H_3 is the well height, and H is the distance from the well center to the nearest node.

The dependence of the average number of iterations N_{iter} on the medium contrast parameter η is presented in Table 1 and Figs. 3, a and b. As we know, the inhomogeneity of the medium entails some increase in the condition number and the number of iterations as evidenced by the presented data.

In Figs. 3, c and d, there are the dependences of the flow rate and average pressure respectively on the parameter η at every time.

In DFM, the fractures are highly permeable voids, and they determine the main direction and density of the fluid flow. Fig. 4 shows the distribution of the pressure field p at the final time depending on η, where at its large values, the main flow goes along the cracks.

5.2. Numerical Experiments for 3D

In the case of three-dimensional simulation, the fractures are represented as two-dimensional planes. When constructing the three-dimensional geometry, the geometry of two-dimensional problem is taken as a basis (Fig. 2, a). The domain is the parallelepiped with sides of 4 km and height of 300 m. The fractures are located vertically in the middle of the domain and have height of 200 m (Fig. 5, a).

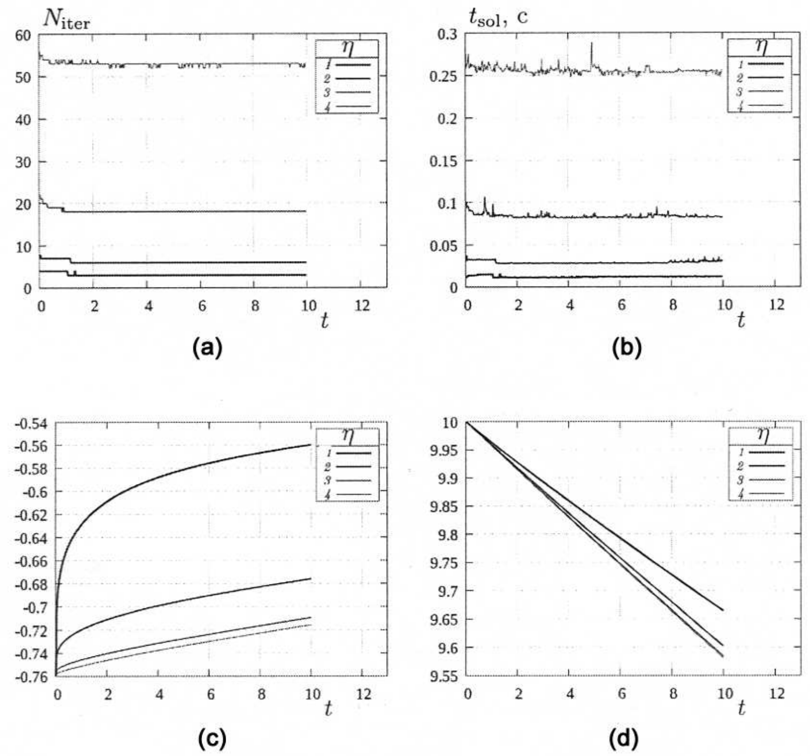

Fig. 3. Number of iterations (a), execution time (b), flow velocity (c), and average pressure (d) in dependence on η.

To study the effect of the parameter η on the solution of the problem, we generate the following two grids with different numbers of nodes and tetrahedral elements:

Grid 1: 720822 nodes and 3759775 elements (Fig. 5, b);

Grid 2: 1621228 nodes and 9358641 elements (Fig. 5, c).

Problem (10)–(13) was solved on the computing cluster NKS-1P of the Siberian Supercomputer Center, 20 nodes with Intel Xeon E5-2697v4 (2.6 GHz, 16 cores) were used. The domain is divided into the subdomains whose number is equal to the number of parallel MPI processes. Table 2 presents the average number of iterations and execution times (in seconds) depending on η, where we observe that the task running on 16 MPI processes shows the faster work. As the number of MPI processes increases, the number of iterations increases, but the execution time required for solving the linear system decreases. It also follows from the results that increasing the number of MPI processes decreases the solution time gap for different parameters of permeability k_f of the fractures.

Fig. 6 shows solutions to the problem at time $t = 1$ year for different values of the parameter η on Grid 2.

CONCLUSION

We considered a discrete fracture model (DFM), which simulates the fractures explicitly. A strong influence of fractures on the fluid flow rate at high values of permeability was shown. The KRYLOV parallel algorithm library was used to solve the SLAE. The direct dependence of the number of iterations

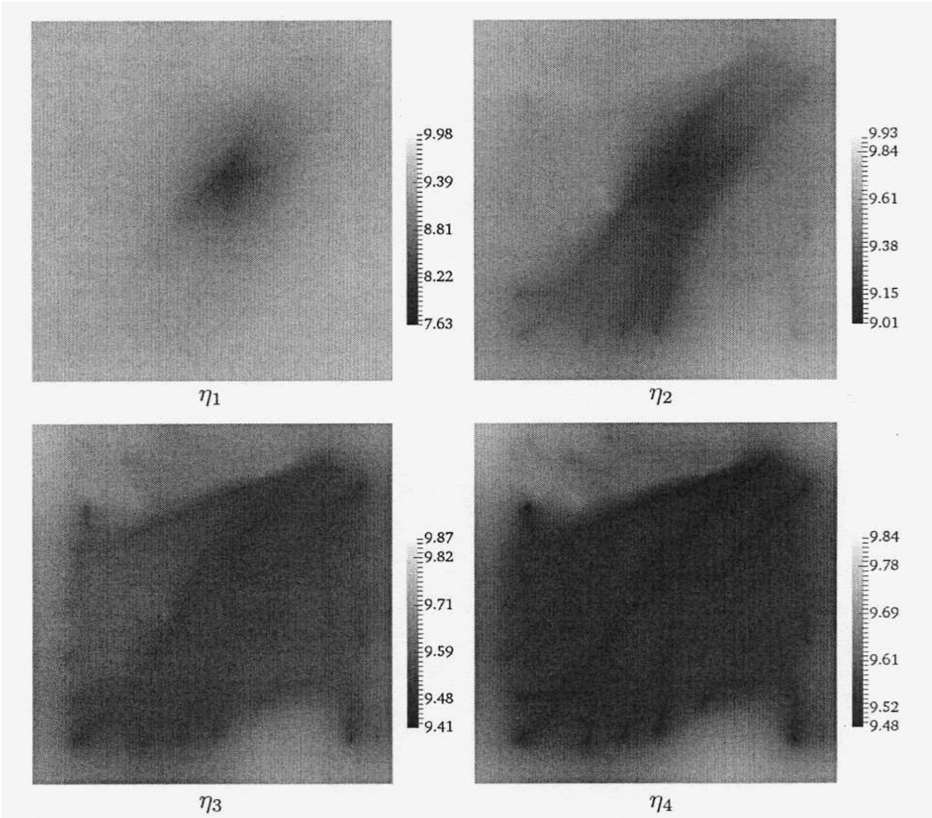

Fig. 4. Pressure distribution at $t = 10$ years.

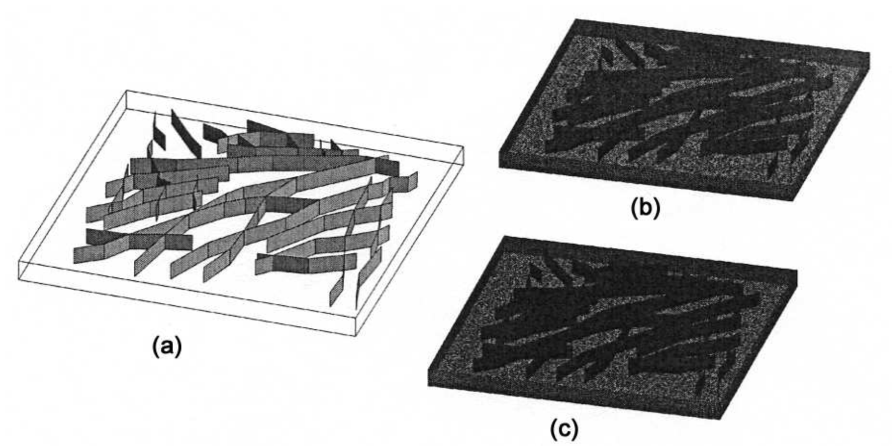

Fig. 5. Geometry of the grid in the $3D$ domain.

and the solution time on the fracture permeability was shown. A numerical study of the effect of the fracture permeability on the convergence of the iterative method for the filtering problem in two-dimensional and three-dimensional productions was carried out.

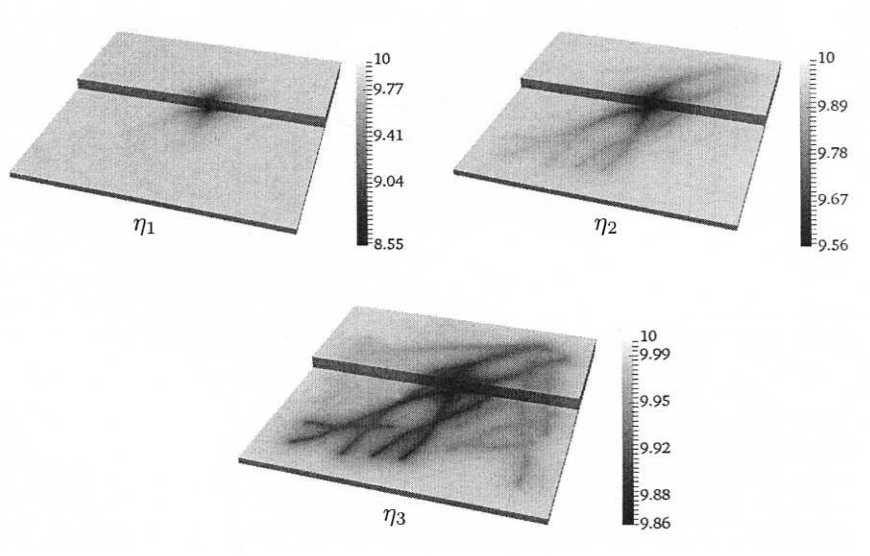

Fig. 6. Pressure distribution at $t = 1$ year on Grid 2 with different η.

Table 2. Average number of iterations $N_{\rm iter}$ and solution time $t_{\rm sol}$ depending on η

Grid	η		Number of processes					
			1	2	4	8	12	16
Сетка 1 $N = 720822$	1	$N_{\rm iter}$	7.31	8.31	19.79	19.82	19.8	19.77
		$t_{\rm sol}$	8.18	2.28	2.67	1.57	1.3	1.2
	2	$N_{\rm iter}$	20.86	20.77	56.35	55.21	54.66	52.72
		$t_{\rm sol}$	22.01	5.71	7.73	3.9	2.79	2.14
	3	$N_{\rm iter}$	63.35	62.01	194.59	191.27	184.71	177.79
		$t_{\rm sol}$	68.1	17.08	27.2	12.7	8.34	5.79
Сетка 2 $N = 1621228$	1	$N_{\rm iter}$	8.47	26.63	30.86	37.82	38.27	37.31
		$t_{\rm sol}$	24.38	19.45	10.01	7.04	6.25	4.34
	2	$N_{\rm iter}$	24.73	33.55	49.28	90.1	91.24	91.37
		$t_{\rm sol}$	67.05	24.03	15.69	16.03	13.42	8.6
	3	$N_{\rm iter}$	73.36	77.76	199.84	564.15	416.8	347.4
		$t_{\rm sol}$	202.03	61.43	65.29	95.24	56.75	28.07

ACKNOWLEDGMENTS

The authors were supported by the Russian Foundation for Basic Research (projects nos. 16–29–15122_ofi_m, 18–01–00295, and 17–01–00732) and by the Megagrant of the Government of the Russian Federation (project no. 14.Y26.31.0013).

REFERENCES

1. G. I. Barenblatt, Yu. P. Zheltov, and I. N. Kochina, "About the Basic Ideas of the Theory of Filtration of Homogeneous Liquids in Fractured Rocks," Prikl. Mat. Mekh. **24** (5), 852–864 (1960).
2. I. Y. Akkutlu, Ya. Efendiev, and M. Vasilyeva, "Multiscale Model Reduction for Shale Gas Transport in Fractured Media," Comput. Geosciences **20** (5), 953–973 (2016).
3. E. T. Chung, Ya. Efendiev, T. Leung, and M. Vasilyeva, "Coupling of Multiscale and Multi-Continuum Approaches," GEM-Internat. J. Geomath. **8** (1), 9–41 (2017).
4. I. Y. Akkutlu, Ya. Efendiev, M. Vasilyeva, and Y. Wang, "Multiscale Model Reduction for Shale Gas Transport in a Coupled Discrete Fracture and Dual-Continuum Porous Media," J. Natural Gas Sci. Engrg. **48**, 65–76 (2017).
5. Ya. Efendiev, S. Lee, L. Guanglian, Ju. Yao, and N. Zhang, "Hierarchical Multiscale Modeling for Flows in Fractured Media Using Generalized Multiscale Finite Element Method," GEM-Internat. J. Geomath. **6** (2), 141–162 (2015).
6. D. T. Snow, "Rock Fracture Spacings, Openings, and Porosities," J. Soil Mech. Found. Div. No. 94, 73–92 (1968).
7. J. Noorishad and M. Mehran, "An Upstream Finite Element Method for Solution of Transient Transport Equation in Fractured Porous Media," Water Resour. Res. No. 18, 588–596 (1982).
8. J. Kim and M. D. Deo, "Comparison of the Performance of A Discrete Fracture Multiphase Model with Those Using Conventional Methods," SPE Symposium on Reservoir Simulation (Houston, 1999), pp. 359–371.
9. J. Kim and M. D. Deo, "Finite Element, Discrete-Fracture Model for Multiphase Flow in Porous Media," AIChE J. No. 46, 1120–1130 (2000).
10. R. Baca, R. Arnett, and D. Langford, "Modeling Fluid Flow in Fractured Porous Rock Masses by Finite Element Techniques," Internat. J. Numer. Methods in Fluids No. 4, 337–348 (1984).
11. Z. Huang, J. Yao, Y. Wang, and K. Tao, "Numerical Study on Two-Phase Flow Through Fractured Porous Media," Science China Technol. Sci. No. 54, 2412–2420 (2011).
12. W. Yu-Shu, G. Qin, R. E. Ewing, Ya. Efendiev, Z. Kang, and Y. Ren, "A Multiple-Continuum Approach for Modeling Multiphase Flow in Naturally Fractured Vuggy Petroleum Reservoirs," in *Internat. Oil and Gas Conference and Exhibition in China*, Vol. 2 (Beijing, 2006), pp. 739–750.
13. W. S. Dershowitz, P. R. La Pointe, and T. W. Doe "Advances in Discrete Fracture Network Modeling," in *Proceedings of US EPA/NGWA Fractured Rock Conference, 2004* (Portland, 2004), pp. 882-894.
14. V. I. Vasiliev, M. V. Vasilyeva, Yu. M. Laevsky, and T. S. Timofeeva, "Numerical Simulation of the Two-Phase Fluid Filtration in Heterogeneous Media," Sibir. Zh. Industr. Mat. **20** (2), 33–40 (2017) [J. Appl. Indust. Math. **11** (2), 289–295 (2017)]. Сиб. журн. индустр. математики. **20** (2), 33–40 (2017).
15. M. M. Karimi-Fard and A. Firoozabadi, "Numerical Simulation of Water Injection in 2D Fractured Media Using Discrete-Fracture Model," SPE REE J. No. 4, 117–126 (2003).
16. V. Dolean, P. Jolivet, and F. Nataf, *An Introduction to Domain Decomposition Methods: Algorithms, Theory and Parallel Implementation* (SIAM, Philadelphia, 2015).
17. D. S. Butyugin, V. P. Il'in, and D. V. Perevozkin, "Methods for Parallel Solution of SLAEs on Systems with Distributed Memory in the Library KRYLOV," Vestnik YuRGU. Ser. Vychisl. Mat. Inform. No. 47(306), 22–36 (2012).
18. D. S. Butyugin, Ya. L. Gur'eva, V. P. Il'in, D. V. Perevozkin, A. V. Petukhov, and I. N.Skopin, "Functionality and Technologies of Algebraic Solvers in the Library KRYLOV," Vestnik YuRGU. Ser. Vychisl. Mat. Inform. **2** (3), 92–105 (2013).
19. V. P. Il'in, "On Incomplete Factorization Methods for Solving Parabolic Equations," Dokl. Akad. Nauk SSSR **318** (6), 1304–1308 (1991).

20. H. P. Langtangen and A. Logg, *Solving PDEs in Python: The FEniCS Tutorial*, Vol. I (Springer, Heidelberg, 2016).
21. J. Li, Z. Lei, G. Qin, and B. Gong, "Effective Local-Global Upscaling of Fractured Reservoirs Under Discrete Fractured Discretization," Energies **8** (9), 10178–10197 (2015).
22. C. Geuzaine and J.-F. Remacle, "Gmsh: A Three-Dimensional Finite Element Mesh Generator with Built in Pre- and Post-Processing Facilities," Internat. J. Numer. Methods in Engrg. **79** (11), 1309–1331 (2009).
23. URL: https://www.s-vfu.ru/universitet/rukovodstvo-i-struktura/instituty/imi/nik_vt/cluster.php
24. M. Vincent, J. Jaffré, and J. E. Roberts, "Modeling Fractures and Barriers as Interfaces for Flow in Porous Media," SIAM J. Scientific Computing. **26** (5), 1667–1691 (2005).
25. J. Yao, Z. Huang, Y. Li, C. Wang, and X. Lu, "Discrete Fracture-Vug Network Model for Modeling Fluid Flow in Fractured Vuggy Porous Media," in *International Oil and Gas Conference and Exhibition in China* (Society of Petroleum Engineers, Beijing, 2010), pp. 320–333.
26. I. Y. Akkutlu, Ya. Efendiev, and M. Vasilyeva, "Multiscale Model Reduction for Shale Gas Transport in Fractured Media," Comput. Geosciences **20** (5), 953–973 (2016).
27. M. Vasilyeva, E. T. Chung, W. T. Leung, and V. Alekseev, "Nonlocal Multicontinuum (NLMC) Upscaling of Mixed Dimensional Coupled Flow Problem for Embedded and Discrete Fracture Models," arXiv preprint arXiv:1805.09407, 2018.
28. I. Y. Akkutlu, Y. Efendiev, M. Vasilyeva, and Y. Wang, "Multiscale Model Reduction for Shale Gas Transport in Poroelastic Fractured Media," J. Comput. Physics No. 353, 356–376 (2018).
29. M. Bukac, I. Yotov, and P. Zunino, "Dimensional Model Reduction for Flow Through Fractures in Poroelastic Media," ESAIM: Mathematical Modelling and Numerical Analysis. **51** (4), 1429–1471 (2017).
30. Z. Chen, G. Huan, and Y. Ma, *Computational Methods for Multiphase Flows in Porous Media* (SIAM, 2006).